Journal of Renewable Materials

Tech Science Press

Doi:10.32604/jrm.2025.02025-0147

ARTICLE

Valorisation of Jicama (*Pachyrhizus erosus*) Bagasse into Cellulose Microfibers for the Reinforcement of Biocomposite Jicama Starch Films

Devita Amelia[1], R. A. Ilyas[1,2,*], Hairul Abral[2,3], Mochamad Asrofi[4], Muhammad Asyraf Muhammad Rizal[2,5], Mohamad Zaki Hassan[6], Mohamad Haafiz Mohamad Kassim[2,7,8], Nurul Fazita Mohammad Rawi[2,7,8], Nasrullah Razali[9] and Melbi Mahardika[2,7,8,10,*]

[1]Faculty of Chemical and Energy Engineering, Universiti Teknologi Malaysia, Skudai, 81310, Johor, Malaysia
[2]Research Collaboration Center for Nanocellulose, BRIN-Andalas University, Padang, 25163, West Sumatera, Indonesia
[3]Department of Mechanical Engineering, Andalas University, Padang, 25163, West Sumatera, Indonesia
[4]Department of Mechanical Engineering, University of Jember, Jember, 68121, Jawa Timur, Indonesia
[5]Engineering Design Research Group (EDRG), Faculty of Mechanical Engineering, Universiti Teknologi Malaysia, Skudai, 81310, Johor, Malaysia
[6]Faculty of Artificial Intelligence, Universiti Teknologi Malaysia, Kuala Lumpur, 54100, Malaysia
[7]Division of Bioresource Technology, School of Industrial Technology, Universiti Sains Malaysia, Gelugor, 11800, Pulau Pinang, Malaysia
[8]Cluster of Green Biopolymer, Coatings & Packaging, School of Industrial Technology, Universiti Sains Malaysia, Gelugor, 11800, Pulau Pinang, Malaysia
[9]Department of Chemical Engineering, Syiah Kuala University, Banda Aceh, 23111, Aceh, Indonesia
[10]Research Center for Biomass and Bioproducts, National Research and Innovation Agency (BRIN), Serpong, South Tangerang, 15314, Banten, Indonesia

*Corresponding Authors: R. A. Ilyas. Email: ahmadilyas@utm.my; Melbi Mahardika. Email: melbi.mahardika@brin.go.id

Received: 17 July 2025; Accepted: 09 October 2025; Published: 24 April 2026

ABSTRACT: This study characterizes biocomposites derived from jicama starch and reinforced with microfibers obtained from jicama bagasse (JB). The incorporation of jicama bagasse microfibers into the jicama matrix was systematically varied at concentrations of 1, 2, 3, 4, and 5 wt%. The starch film and biocomposite were prepared using solution casting methodologies, employing glycerol as a plasticizing agent. The biocomposites were characterized using Fourier-transform infrared spectroscopy, X-ray diffraction analysis, and scanning electron microscopy. In addition, the moisture absorption and tensile properties were evaluated. The jicama starch contained 44% w/w amylose, whereas the jicama bagasse microfiber contained 55.98% w/w cellulose. Following the incorporation of jicama bagasse microfibers at concentrations ranging from 1 to 3 wt%, the biocomposite film exhibited a statistically significant enhancement ($p \leq 0.05$) in its tensile properties and moisture resistance. The biocomposite containing 3 wt% jicama bagasse microfiber exhibited the most favorable properties. Specifically, the tensile strength, crystallinity index, and moisture absorption (after 6 h) of this film were recorded at 9.7 MPa (an increase of 470%), 6.7% (an increase of 14.7%), and 32.6% (a decrease of 31.6%), respectively, in comparison to the pure starch film. These findings indicate that the biocomposite film has considerable potential for application in industrial food packaging.

KEYWORDS: Biocomposite; jicama starch; microfibers; tensile properties

Copyright © 2026 The Authors. Published by Tech Science Press.
This work is licensed under a Creative Commons Attribution 4.0 International License, which permits unrestricted use, distribution, and reproduction in any medium, provided the original work is properly cited.

1 Introduction

Conventional plastics derived from petroleum are non-renewable and pose significant environmental hazards due to their non-biodegradable nature and accumulation in ecosystems [1–4]. Consequently, the development of sustainable and biodegradable alternatives has become a major focus in material science. Among these alternatives, starch-based bioplastics have gained considerable attention due to their biodegradability, renewability, low cost, and ease of processing [5].

Starch is a natural polysaccharide widely available from various plant sources, including cassava [6], corn [7], potato [8], and jicama [9]. Typically, cassava and corn starch are most commonly used in biocomposite production [10]. Another promising starch source in tropical countries, particularly Indonesia, is jicama (*Pachyrhizus erosus*), as it is widely available, grows rapidly in hot and humid climates, and yields a high starch content [9]. However, pure starch-based films generally suffer from high moisture sensitivity and poor mechanical strength, limiting their practical applications, especially in packaging [11]. To overcome these shortcomings, the incorporation of fillers or reinforcing agents into the starch matrix is a common strategy to enhance its mechanical and barrier properties [12].

Natural fibers are considered effective reinforcement agents due to their biodegradability, abundance, and favorable mechanical characteristics [13–17]. These fibers mainly consist of cellulose, hemicellulose, lignin, and minor extractives [18,19]. Chemical treatments, such as alkalization and bleaching, are often applied to remove non-cellulosic components and improve fiber-matrix compatibility [18]. Various natural fibers have been successfully employed to reinforce starch-based films, including pineapple leaf fibers [20], sugarcane bagasse fibers [21], bacterial cellulose [22], and cassava pulp fiber [23].

Previous research has demonstrated that the addition of cellulose micro/nanofibers derived from agro-industrial waste significantly improves biocomposite properties. For example, Teixeira et al. (2009) reported enhanced crystallinity, thermal stability, and mechanical strength in cassava starch films reinforced with cellulose extracted from cassava bagasse [24]. Similarly, Gilfillan et al. (2014) observed increased tensile strength and reduced water absorption in potato starch films reinforced with sugarcane bagasse nanofibers [25]. These findings underscore the potential of agro-waste-derived fibers for sustainable material development.

In this study, the reinforcing potential of jicama bagasse microfibers (JBM) in jicama starch (JS) films was investigated. Unlike previous studies that focused on cellulose extraction, this study utilized jicama bagasse fibers directly after drying and mechanical grinding, without extensive chemical purification. The structural, mechanical, and moisture barrier properties of the JS films reinforced with varying JBM contents were evaluated and analyzed statistically. This approach explores a valorization pathway for jicama agricultural residue as a low-cost, eco-friendly reinforcing agent for biodegradable films.

2 Materials and Methods

2.1 Materials

Fresh jicama tubers (*Pachyrhizus erosus*) were obtained from a local agricultural facility in Bogor, West Java, Indonesia. These tubers served as the primary sources of both starch and microfibers. All chemicals used for the analysis of jicama bagasse microfiber composition and the determination of amylose content in jicama starch were purchased from Sigma-Aldrich and used without further modification. Glycerol (≥99.5% purity) was purchased from Sigma-Aldrich (Jakarta, Indonesia) and used as a plasticizer agent, and distilled water was purchased from CV. Mulia Jaya (Bogor, Indonesia).

2.2 Extraction of Jicama Starch (JS)

The jicama tubers were peeled and cut into approximately 20 mm pieces. Extraction was carried out using a slow-speed juicer (SKG Slow Juicer, Indonesia), resulting in a suspension containing both jicama starch and moist bagasse. The suspension was filtered through a 200T mesh screen (74 μm) to separate the residual bagasse from the starch slurry. After settling for 20 h, the supernatant starch suspension was decanted from the sediment. The obtained wet starch was then dried in a ventilated oven (Memmert, Germany, Model UN 55) at 50°C until a constant weight was achieved.

2.3 Preparation of Jicama Bagasse Microfibers (JBM)

The moist jicama bagasse was oven-dried at 60°C for 12 h in a ventilated drying oven. The dried material was then ground using a high-speed blender (Philips, 12,000 rpm) for 30 min. The ground jicama bagasse was subsequently sieved through a 200T mesh (74 μm) to obtain a uniform particle size, and the resulting powder was referred to as JBM.

2.4 Preparation of Jicama Starch Film and Biocomposites

Approximately 10 g of jicama starch (JS) powder was solubilized in 100 mL of distilled water. The JBM was incorporated into the suspension at varying loading (1–5 wt%). Subsequently, the solution was treated with a high-shear homogenizer (Ultra Turrax, T25, IKA, Germany) at 12,000 rpm for 5 min at ambient temperature. Approximately 2% (v/v) glycerol was introduced into the mixture, which was then heated using a hot plate magnetic stirrer (Daihan Scientific) at temperatures ranging from 75°C to 80°C for 10 min until complete gelatinization was achieved [9]. After gelatinization, the suspension was cast into a glass mold (200 mm × 150 mm) and dried at 50°C for 24 h [20]. Table 1 shows the ratios of starch, fiber, and other ingredients used with the labeling key for each sample.

Table 1: Amounts of starch, fiber, and other ingredients used with the labeling key for each sample

Sample	JS (g)	Dried JBM (wt%)	Distilled water (mL)	Glycerol (mL)
JS film	10	–	100	2
JS-1JBM	10	1	100	2
JS-2JBM	10	2	100	2
JS-3JBM	10	3	100	2
JS-4JBM	10	4	100	2
JS-5JBM	10	5	100	2

2.5 Chemical Composition of Jicama Baggasse Fiber and Jicama Starch

The chemical composition of JBM was assessed using TAPPI Standard T 9 M-54 for the quantification of cellulose, TAPPI Standard T 13 m-54 for the determination of lignin, and ASTM 1104-56 for holocellulose analysis. The amylose and amylopectin content of JS was evaluated according to McGrane's methodology, which is based on the calorimetric analysis of iodine complexes with specific modifications [26]. Desiccated JS was prepared and dried in an oven at 60°C for 20 h. A mass of 0.1 g of dried JS was combined with 1 mL of ethanol (95%) and 9 mL of sodium hydroxide (1 N) in a test tube. The mixture was heated in a water bath at 85°C for 10 min to facilitate gelatinization. Following this, the solution was transferred to a volumetric flask, agitated, and distilled water was added to achieve a final volume of 100 mL. An aliquot of 5 mL from this mixture was combined with 1 mL of acetic acid (1 N), 2 mL of iodine solution, and distilled water to

a total volume of 100 mL. The resultant solution was agitated and allowed to rest for 20 min. Thereafter, it was analyzed using a UV-vis spectrophotometer (Shimadzu UV 1800, Japan) at a wavelength of 625 nm, employing a 1 cm path length quartz cell to ascertain the absorbance value. From this absorbance value, the proportions of amylose and amylopectin can be accurately determined.

2.6 Characterization

2.6.1 Tensile Tests

The tensile characteristics of the JS film and biocomposite were systematically examined using a COM-TEN series 95TS5K tensile testing apparatus. The tensile testing rate was set at 5 mm/min. Tensile specimens were prepared with dimensions of 100 mm × 10 mm × 0.1 mm in accordance with the ASTM D882-12 standard. The evaluation process was conducted five times for each sample.

2.6.2 X-Ray Diffraction (XRD)

X-ray diffraction (XRD) analysis of the JS film and biocomposites was conducted using an X'Pert PROPAN alytical apparatus (Philips Analytical, Almelo, The Netherlands). The specimens were scanned across the angular range of 2θ = 5° to 50° employing CuKα radiation (λ = 0.154) at operational parameters of 40 kV and 30 mA. Before XRD analysis, the samples were dried in an oven at 60°C for 2 h. The crystallinity index (CI) of the sample was determined using the following equation (Eq. (1)) [27].

$$CI = \left[\left(I_{002} - I_{am}\right)/I_{002}\right] \times 100 \quad (1)$$

In this equation, I_{002} denotes the intensity measured at 2θ = 22.6°, which corresponds to the crystalline phase, whereas I_{am} represents the intensity recorded at 2θ = 18°, indicative of the amorphous phase.

2.6.3 Morphological Observation

The JS film and biocomposites were deposited onto the Scanning Electron Microscopy (SEM) sample stub. A 30-s gold coating was applied to the film to mitigate the accumulation of electron charge. The surface morphology of the JBM, along with the surface fractures of the JS film and biocomposite, was examined using SEM (Hitachi series 3400 N, Japan) at an acceleration voltage of 15 kV.

2.6.4 Fourier Transform Infrared Spectroscopy (FTIR)

An FTIR spectrometer (Frontier, Perkin Elmer, USA) was used to analyze the FTIR spectra of the JS film and biocomposites. The scanning process was conducted within the wavenumber range of 4000–600 cm^{-1}, maintaining a resolution of 4 cm^{-1}.

2.6.5 Moisture Absorption

The moisture absorption (MA) of the samples was measured following the procedure described in a previous study [20,28], with slight modifications. The JS films and biocomposites were carefully cut into rectangular specimens measuring 1 cm × 1.5 cm and dried in a ventilated oven (Universal Oven Memmert) until a constant weight was achieved. Distilled water was placed in a sealed chamber to maintain a relative humidity (RH) of 99%. The dried specimens were then placed inside the chamber at 25°C for 6 h. The weight of each specimen was recorded every 30 min using a precision balance with an accuracy of 0.1 mg (Kenko). The moisture absorption percentage was determined using Eq. (2):

$$\text{Moisture absorption}(\%) = \left(\left(wt - w_0\right)\right)/w_0 \times 100 \quad (2)$$

where w_0 represents the initial weight and w_t denotes the final weight of the specimen.

2.6.6 Statistical Analysis

The significance of variations in tensile characteristics and moisture uptake across various jicama bagasse microfiber loadings within the biocomposite film was assessed using analysis of variance (ANOVA). Upon identifying significant differences at $p \leq 0.05$, a subsequent examination was performed using Duncan's multiple-range test.

3 Results and Discussions

3.1 Chemical Composition of Jicama Bagasse Microfiber and Jicama Starch

Chemical composition analysis was used to measure the cellulose, hemicellulose, lignin, and extractive content of the fiber. Jicama bagasse microfiber (JBM) contained 55.9% w/w cellulose, 77.8% w/w holocellulose, 21.8% w/w hemicellulose, 2.6% w/w lignin, and 3.9% w/w extractive content, respectively. This cellulose content value is higher than that found in raw rice straw fibers [29], indicating that JBM may be more practical as reinforcement in biocomposites, due to its high cellulose content, which contributes to improved mechanical properties. Jicama starch (JS) had amylose and amylopectin contents of 44% w/w and 56% w/w, respectively. The amylose content of JS is higher than that of other starch resources, such as cassava starch (13%–29% w/w amylose) [30], potato (10.49%–20.48% w/w amylose) [31], sago (21.4%–30.0% w/w amylose) [32], and corn (27.5% w/w amylose) [33]. Amylose content is affected by factors such as variety, age of the plant, soil humidity, and water content [34,35]. High amylose content in starch-based films results in superior mechanical properties [36].

3.2 Tensile Properties

Fig. 1 shows the tensile strength (TS), tensile modulus (TM), and elongation at break (EB) of both pure JS and biocomposite films. The pure JS film exhibited the lowest TS (1.5 MPa) and TM (20.9 MPa). The incorporation of JBM into the JS matrix significantly enhanced the mechanical properties of the film. Both TS and TM increased sharply with the addition of JBM, reaching peak values at the JS-3JBM composition—approximately 9.8 MPa for TS and 440 MPa for TM. The increased stiffness was attributed to the good dispersion and high compatibility of JBM within the starch matrix. The formation of hydrogen bonds between the hydroxyl (–OH) groups of the microfibers and starch contributes to the formation of a denser, more rigid network, thereby strengthening the film structure. This result is supported by the FTIR analysis results [37]. Additionally, Fig. 1c shows that the decrease in EB observed for this composition is attributed to the increased film stiffness, which limits the polymer chain mobility within the matrix [38]. Different lowercase letters above the bars in Fig. 1 indicate statistically significant differences among the mean values according to Duncan's multiple range test at $p < 0.05$. The TS of the JS biocomposite (JS-3JBM) was six times higher than that of cassava starch-based biocomposite films reinforced with 10 wt% luffa fibers [39] and 69% higher than that of biocomposites made from potato starch reinforced with nanofiber sugarcane bagasse [25].

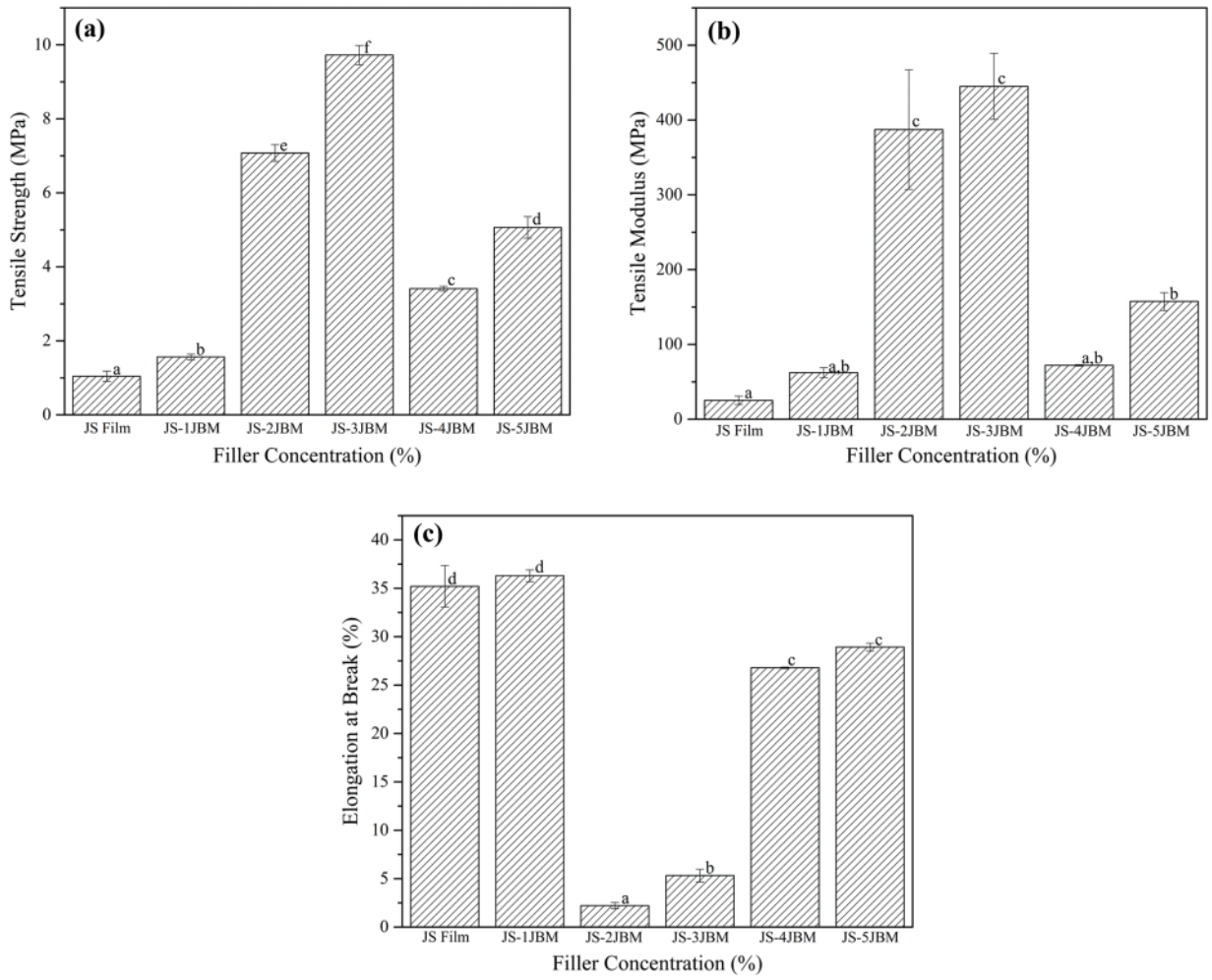


Figure 1: Tensile properties of the films at different filler concentrations: (**a**) tensile strength, (**b**) tensile modulus, and (**c**) elongation at break. Error bars represent standard deviations. Different lowercase letters (**a**–**f**) above the bars indicate statistically significant differences among the means according to Duncan's multiple range test at $p < 0.05$

The significant decrease in TS and TM observed in JS-4JBM compared with JS-3JBM was due to the addition of JBM beyond the optimal amount. When the JBM concentration is too high, the filler particles tend to agglomerate owing to stronger interactions between the particles than with the matrix [40]. This agglomeration resulted in an uneven distribution of fillers and the formation of weak points within the film structure. Consequently, the system's ability to efficiently transfer stress is reduced [41]. Moreover, a high filler concentration can lead to the formation of microvoids that disrupt the structural continuity of the film and weaken the interfacial adhesion between the filler and matrix [40,41]. The incomplete wetting of the filler by the matrix at high concentrations can also hinder the formation of strong interfacial bonds, ultimately reducing the overall mechanical integrity of the film [42]. Interestingly, although TS and TM decreased in JS-4JBM, EB significantly increased compared with JS-3JBM. This increase indicates a recovery in the film's flexibility and ductility, likely caused by a reduction in the filler network density due to agglomeration, which allows for increased polymer chain mobility [41,43]. In other words, despite the weakened structure, the film tends to be more flexible due to the loss of internal stiffness previously formed by the optimal filler distribution.

At JS-5JBM, the recoveries of TS and TM were observed; however, the values did not reach the optimal performance of JS-3JBM. This improvement was due to the partial redistribution of the filler and the filling of microvoids by additional JBM particles. This process enhances local adhesion and improves the stress transfer pathways within the matrix [44,45]. Although agglomeration is still evident in the SEM images of the JS-5JBM structure, the combination of well-dispersed particles and filled interstitial gaps enables the film to regain some strength and stiffness. Thus, the EB remains high, indicating that, despite the filler network not being as optimal as that in JS-3JBM, the JS-5JBM film can maintain better flexibility. A similar phenomenon was reported by Khalili et al. (2023), who found that adding cellulose nanocrystals (CNCs) up to 20% into a starch matrix increased EB by 52% due to the synergy between the helical layered structure of CNCs, the flexible matrix, and effective interfacial adhesion [46]. Therefore, although agglomeration is unavoidable at high concentrations, a higher JBM content can still contribute to reinforcement by filling void spaces and increasing the composite network density while maintaining or even enhancing the film ductility.

3.3 XRD Pattern

Fig. 2 shows the XRD patterns of the starch film (JS) and JS-JBM biocomposites used to evaluate the crystalline structure of the materials. The pure JS film exhibited low-intensity diffraction peaks, indicating the dominance of an amorphous structure. This result can be attributed to the starch gelatinization process and the use of plasticizers, which disrupt the regularity of the crystalline arrangement [47,48]. However, after the addition of JBM, the diffraction intensity increased significantly, especially in JS-3JBM and JS-5JBM, with the appearance of a peak at approximately $2\theta = 22.5°$, indicating an increase in structural order owing to the presence of JBM as a crystalline component. This result is consistent with the crystallinity index (CI) data in Table 2, where the CI increased from 5.9% (JS film) to 6.7% (JS-3JBM) and 6.9% (JS-5JBM), showing that JBM acts as a crystal nucleation site that promotes the formation of a more stable semi-crystalline structure within the starch matrix. This increase in crystallinity is also supported by the FTIR absorbance ratio at 995/1022 cm^{-1}, which increased from 82.2 in JS to 86.5 in JS-3JBM, indicating an enhanced polymer chain ordering. The higher structural order contributes to increased stiffness and mechanical strength of the film, as reflected in the highest TM and TS values observed for JS-3JBM [47]. However, although JS-5JBM exhibited a higher crystallinity index, its mechanical performance did not surpass that of JS-3JBM. This phenomenon is likely due to the agglomeration of JBM particles at high concentrations, which disrupts the continuity and interfacial cohesion within the film, as observed in the SEM images (Fig. 3d) [45,49]. Therefore, although the addition of JBM enhances the crystallinity and structural order, these positive effects depend heavily on the homogeneity of the JBM dispersion within the matrix. This finding is consistent with previous reports indicating that increased crystallinity from cellulose addition can reinforce the structure of biocomposite films, but only when the particle dispersion is uniform [50].

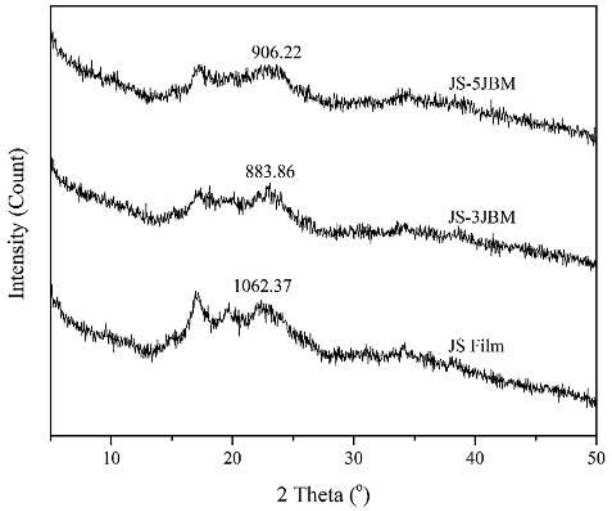


Figure 2: XRD patterns of the starch film and biocomposites

Table 2: Crystallinity index and absorbance ratio bands at 995 and 1022 cm^{-1} of starch films and biocomposites

Sample	CI (%)	Absorbance ratio bands of 995/1022 (%)
JS film	5.9	82.2
JS-3JBM	6.7	86.5
JS-5JBM	6.9	83.3

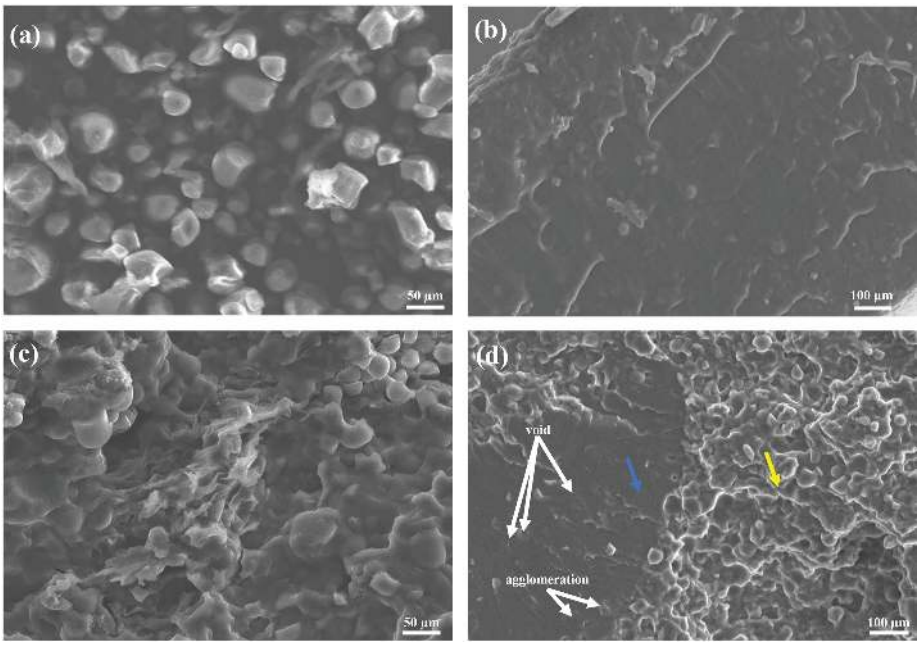


Figure 3: SEM images of granule starch and fracture surface for (**a**) JBM, (**b**) JS film, (**c**) JS-3JBM, and (**d**) JS-5JBM

3.4 Morphology of JBM and Fracture Surface

SEM photographs of the JBM particles and fracture surfaces of the JS film and biocomposites from the tensile testing are displayed in Fig. 3. Fig. 3a shows that JBM has a rough surface with clearly visible microfibrillar structures and particle diameters ranging from 3.04 to 10.1 μm. The rough and microfibrillar surface morphology provides more interfacial contact area and enhances mechanical interlocking with the starch matrix, which is widely recognized as a key factor contributing to effective stress transfer in biocomposites [51,52]. Therefore, JBM shows strong potential as a reinforcing agent in starch matrix. SEM micrographs of the fracture surface of the pure JS film (Fig. 3b) reveal a dense and smooth surface without large pores or cracks. This morphology indicates that the film has a compact structure but tends to be brittle due to the absence of a reinforcing network, consistent with mechanical testing results showing low TS and TM. The addition of JBM to the JS film influenced the fracture surface morphology of the JS-JBM biocomposite films. Fig. 3c,d displays the fracture surface morphology of JS-JBM films after the incorporation of different JBM concentrations (3 and 5 wt%). The surface morphology varied depending on the composition of the composite. Fig. 3c (JS-3JBM) shows a rougher and more irregular fracture surface with well-dispersed JBM particles in the matrix. This structure suggests good interfacial interactions between the JBM and starch, as well as the formation of a cohesive reinforcing network [47]. The heterogeneous fracture surface indicates that more energy is required to cause damage, which correlates with the increased tensile strength and modulus observed in this formulation. Fig. 3d (JS-5JBM) exhibits two distinct morphological characteristics: the left side (blue arrow) shows a relatively smooth surface, indicating a brittle fracture or weak planes caused by agglomeration, whereas the right side (yellow arrow) displays a rough and irregular area associated with the accumulation of poorly dispersed JBM particles. In addition, voids and agglomerated regions are highlighted by white arrows. These features confirm that agglomeration hinders matrix wetting, promotes microvoid formation, and reduces the stress transfer efficiency within the system [42]. Although JS-5JBM shows some mechanical property recovery compared to JS-4JBM, its performance remains lower than that of JS-3JBM because of structural heterogeneity.

3.5 FTIR Spectra

Fig. 4 shows the FTIR spectra illustrating the interactions between the starch extracted from JS and JBM, as well as the chemical structure of the resulting biocomposite films. All samples exhibited similar characteristic peaks, which can be attributed to the comparable chemical structures of starch and microfibers. The broad absorption band at 3303 cm^{-1} is associated with –OH stretching vibrations, the band at 2927 cm^{-1} corresponds to C–H stretching, and the band at 1640 cm^{-1} originates from C–O stretching vibrations [28,39]. A change was observed in the –OH stretching vibration at 3303 cm^{-1}, where the transmittance increased from 21.7% in the pure starch film to 24.8% in the starch-microfiber biocomposite film (JS-3JBM). At JS-5JBM, the transmittance value decreased to 22.1% but remained higher than that of the pure film (see Fig. 4). This result indicates a decrease in the intensity of the –OH groups due to a reduction in hydrogen bonding between the starch chains, as some –OH groups of starch interact with the –OH groups from the microfibers. Consequently, an interfacial interaction is formed between the starch and microfibers, which restricts the starch chain mobility [49]. This condition reduces the film's ability to absorb water, as evidenced by the decreased intensity of the C–O stretching band at 1640 cm^{-1}, indicating a reduced amount of bound water within the film matrix. These results align with previous studies reporting that the addition of cellulose microfibers and cellulose nanocrystals into starch matrices reduces the intensity of the –OH stretching band (3350–3254 cm^{-1}) [46]. Similarly, the reduction in absorption intensity at 1640 cm^{-1} (C–O stretching) correlates directly with the decreased water-binding capacity in starch-based matrices due to the presence of cellulose fillers [53]. Overall, the FTIR results demonstrate that the incorporation of JBM into the JS matrix

causes (i) a shift in hydrogen bonding from starch–starch interactions to starch–JBM interactions and (ii) a decrease in the film's affinity toward water molecules. This suggests that the extracted JBM was well integrated into the JS matrix, forming a homogeneous and stable composite.

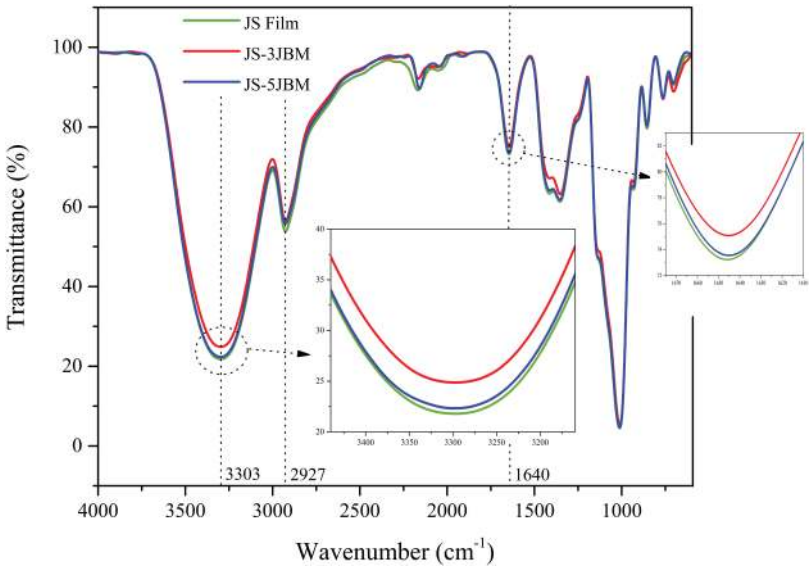


Figure 4: FTIR spectra of the starch film and biocomposites

3.6 Moisture Absorption

Fig. 5 shows the moisture absorption (MA) of the pure starch film and biocomposites with the addition of JBM. The pure starch film exhibited the highest moisture absorption of 47.7% after 6 h in the humidity chamber. The presence of JBM in the starch matrix decreased the moisture absorption. For example, the addition of 3 wt% JBM reduced MA by 31.6%. The increase in JBM in the matrix significantly reduced moisture absorption ($p \leq 0.05$) owing to the higher hydrophobicity of JBM. The homogeneous distribution and decrease in free hydroxyl groups in JS-3JBM also contributed to the decreased MA. A similar result was reported in a previous study [28]. The water vapor uptake measurements of the JS-3JBM sample showed the best water resistance. This result is still 30% lower than that of biocomposite films made from maize starch reinforced with 10% nanofiber from kenaf bast [7].

In the case of JS-5JBM, the moisture absorption (MA) value increased to 42%, which is higher than that of JS-3JBM (31.6%). This increase in MA can be attributed to the presence of microvoids formed in the matrix owing to the higher cellulose content [54]. These microvoids provide additional space that can trap water molecules, leading to an increase in MA. However, MA remains lower than that of the pure starch film (47%) due to the addition of cellulose, which reduces the number of free –OH groups and increases intermolecular bonding, thereby limiting water penetration (as shown in Fig. 4) [54]. Although the formation of microvoids slightly increases MA, this effect does not outweigh the overall barrier effect of cellulose, which contributes to enhancing the water resistance of the biocomposite [55].

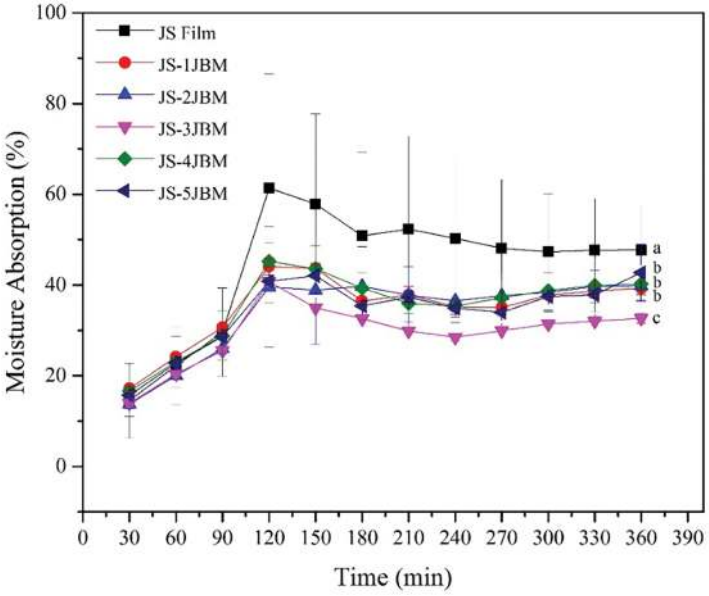


Figure 5: Average moisture absorption of each film

4 Conclusions

This study successfully developed jicama starch (JS)-based biocomposite films reinforced with jicama bagasse microfibers (JBM), demonstrating significant improvements in their structural and mechanical properties. The JS-3JBM formulation exhibited the best performance compared to the neat jicama starch (JS) film, showing remarkable enhancements of 470% in tensile strength, 1905% in tensile modulus, and 13.56% in crystallinity index, along with a 31.6% reduction in moisture absorption due to excellent starch-microfiber interfacial adhesion. Therefore, this study highlights the promising features of biocomposite films with micrometer-scale structures and paves the way for the development of food packaging materials with enhanced and optimized performance.

Acknowledgement: The authors acknowledge financial support from the Degree by Research (DBR) program, National Research and Innovation Agency of Indonesia (BRIN), which funded the doctoral research of one of the authors. The authors also acknowledge the facilities and scientific and technical support provided by the Advanced Characterization Laboratories Cibinong–Integrated Laboratory of Bioproducts, the Advanced Characterization Laboratories Serpong, and the Cryo-EM Laboratory–Aquilos 2, National Research and Innovation Agency (BRIN), through E-Layanan Sains, Badan Riset dan Inovasi Nasional.

Funding Statement: This work was financially supported by BRIN through the project 'RIIM Kompetensi Gelombang 7', under grant number 61/II.7/HK/2024.

Author Contributions: Conceptualization, data curation, project administration, funding acquisition, and supervision: Melbi Mahardika. Writing—original draft: Melbi Mahardika and Devita Amelia. Research assistant and investigation in laboratory: Melbi Mahardika, Devita Amelia. Formal analysis and writing—review and editing: Hairul Abral, Mochamad Asrofi, Muhammad Asyraf Muhammad Rizal, Mohamad Zaki Hassan, Mohamad Haafiz Mohamad Kassim. Supervision and validation: R. A. Ilyas. Resources: Nurul Fazita Mohammad Rawi and Nasrullah Razali. All authors reviewed the results and approved the final version of the manuscript.

Availability of Data and Materials: The detailed data obtained through this study and presented in this article can be requested from the corresponding authors.

Ethics Approval: Not applicable.

Conflicts of Interest: The authors declare no conflicts of interest to report regarding the present study.

References

1. Prasanna Kumar M, Vijayakumar A, Govindarasu P, Murdamootoo J, Lavanya P, Ramkumar R, et al. Replacement of conventional packaging materials with green polymers. In: Islam SU, Shahid M, editors. Green materials for active food packaging. Singapore: Springer Nature; 2025. p. 197–227. doi:10.1007/978-981-96-0369-5_6.
2. Choudhury BK, Haloi R, Bharadwaj KK, Rajkhowa S, Sarma J. Bio-based and biodegradable plastics as alternatives to conventional plastics. Plast Microplastic Environ Manag Health Risks. 2022;23(1):170–86. doi:10.1002/9781119800897.ch9.
3. Rajendran S, Al-Samydai A, Palani G, Trilaksana H, Sathish T, Giri J, et al. Replacement of petroleum based products with plant-based materials, green and sustainable energy—a review. Eng Rep. 2025;7(4):e70108. doi:10.1002/eng2.70108.
4. Sharma D, Moondra N, Bharatee RK, Nema A, Sweta K, Yadav MK, et al. Processing and recycling of plastic wastes for sustainable material management. Plast Waste Manag. 2024:89–116. doi:10.1002/9783527842209.ch4.
5. Yu X, Chen L, Jin Z, Jiao A. Research progress of starch-based biodegradable materials: a review. J Mater Sci. 2021;56(19):11187–208. doi:10.1007/s10853-021-06063-1.
6. Müller CMO, Borges J, Yamashita F. Composites of thermoplastic starch and nanoclays produced by extrusion and thermopressing. Carbohydr Polym. 2012;89(2):504–10. doi:10.1016/j.carbpol.2012.03.035.
7. Karimi S, Dufresne A, Md Tahir P, Karimi A, Abdulkhani A. Biodegradable starch-based composites: effect of micro and nanoreinforcements on composite properties. J Mater Sci. 2014;49(13):4513–21. doi:10.1007/s10853-014-8151-1.
8. Balakrishnan P, Gopi S, Thomas S. UV resistant transparent bionanocomposite films based on potato starch/cellulose for sustainable packaging. Starch-Stärke. 2018;70(1–2):1700139. doi:10.1002/star.201700139.
9. Abral H, Soni Satria R, Mahardika M, Hafizulhaq F, Affi J, Asrofi M, et al. Comparative study of the physical and tensile properties of jicama (*Pachyrhizus erosus*) starch film prepared using three different methods. Starch-Stärke. 2019;2019:1–31. doi:10.1002/star.201800224.
10. Bangar SP, Dhull SB, Manzoor M, Chandak A, Esua OJ. Functionality and applications of non-conventional starches from different sources. Starch-Stärke. 2024;76(1–2):2300073. doi:10.1002/star.202300073.
11. Arruda TR, Machado GD, Marques CS, Souza AL, Pelissari FM, Oliveira TV, et al. An overview of starch-based materials for sustainable food packaging: recent advances, limitations, and perspectives. Macromol. 2025;5(2):19. doi:10.3390/macromol5020019.
12. Muñoz-Gimena PF, Oliver-Cuenca V, Peponi L, López D. A review on reinforcements and additives in starch-based composites for food packaging. Polymers. 2023;15(13):2972. doi:10.3390/polym15132972.
13. Dutta D, Sit N. Preparation and characterization of potato starch-based composite films reinforced by modified banana fibers and its application in packaging of grapes. Int J Biol Macromol. 2024;2023:127791. doi:10.1016/j.ijbiomac.2023.127791.
14. Tian J, Kong Y, Qian S, Zhang Z, Xia Y, Li Z. Mechanically robust multifunctional starch films reinforced by surface-tailored nanofibrillated cellulose. Compos Part B Eng. 2024;275(7844):111339. doi:10.1016/j.compositesb.2024.111339.
15. Boroujeni FM, Fioravanti G, Kander R. Synthesis and characterization of cellulose microfibril-reinforced polyvinyl alcohol biodegradable composites. Materials. 2024;17(2):526. doi:10.3390/ma17020526.
16. Huang X, Xie F, Xiong X. Surface-modified microcrystalline cellulose for reinforcement of chitosan film. Carbohydr Polym. 2018;201(17):367–73. doi:10.1016/j.carbpol.2018.08.085.
17. Tang C, Liu H. Cellulose nanofiber reinforced poly (vinyl alcohol) composite film with high visible light transmittance. Compos Part A Appl Sci Manuf. 2008;39(10):1638–43. doi:10.1016/j.compositesa.2008.07.005.

18. Ali Z, Talpur FN, Afridi HI, Ahmed F, Brohi NA, Abbasi H. Analytical approaches and advancement in the analysis of natural and synthetic fiber: a comprehensive review. Spectrochim Acta Part A Mol Biomol Spectrosc. 2025;326:125164.
19. Pratama AW, Mahardika M, Widiastuti N, Piluharto B, Ilyas RA, Sapuan SM, et al. Isolation and characterization of highly thermal stable microcrystalline cellulose derived from belulang grass (*Eleusine indica*). Case Stud Chem Env Eng. 2024;9:100743. doi:10.1016/j.cscee.2024.100743.
20. Mahardika M, Abral H, Kasim A, Arief S, Hafizulhaq F, Asrofi M. Properties of cellulose nanofiber/bengkoang starch bionanocomposites: effect of fiber loading. LWT. 2019;116(8):108554. doi:10.1016/j.lwt.2019.108554.
21. Nyerere G, Kyokusiima S, Nabaterega R, Tumusiime G, Kavuma C. The synergy of maize straw cellulose and sugarcane bagasse fibre on the characteristics of bioplastic packaging film. Bioresour Technol Rep. 2024;28(6):102007. doi:10.1016/j.biteb.2024.102007.
22. Ghozali M, Meliana Y, Masruchin N, Rusmana D, Chalid M. Preparation and characterization of *Arenga pinnata* thermoplastic starch/bacterial cellulose nanofiber biocomposites via *in-situ* twin screw extrusion. Int J Biol Macromol. 2024;261:129792. doi:10.1016/j.ijbiomac.2024.129792.
23. Jeencham R, Chiaoketwit N, Numpaisal P, Ruksakulpiwat Y. Study of biocomposite films based on cassava starch and microcrystalline cellulose derived from cassava pulp for potential medical packaging applications. Appl Sci. 2024;14(10):4242. doi:10.3390/app14104242.
24. Teixeira EDM, Pasquini D, Curvelo AAS, Corradini E, Belgacem MN, Dufresne A. Cassava bagasse cellulose nanofibrils reinforced thermoplastic cassava starch. Carbohydr Polym. 2009;78:422–31. doi:10.1016/j.carbpol.2009.04.034.
25. Gilfillan WN, Moghaddam L, Doherty WOS. Preparation and characterization of composites from starch with sugarcane bagasse nanofibres. Cellulose. 2014;21:2695–712. doi:10.1007/s10570-014-0277-4.
26. McGrance SJ, Cornell HJ, Rix CJ. A simple and rapid colorimetric method for the determination of amylose in starch products. Starch-Stärke. 1998;50:158–63.
27. Segal L, Creely JJ, Martin AE, Conrad CM. An empirical method for estimating the degree of crystallinity of native cellulose using the X-ray diffractometer. Text Res J. 1959;29:786–94. doi:10.1177/004051755902901003.
28. Asrofi M, Abral H, Kasim A, Pratoto A, Mahardika M, Hafizulhaq F. Characterization of the sonicated yam bean starch bionanocomposites reinforced by nanocellulose water hyacinth fiber (whf): the effect of various fiber loading. J Eng Sci Technol. 2018;13:2700–15.
29. Islam M, Sinha ASK, Prasad K. Organosolv delignification of rice straw cellulose fiber for functional food packaging. Cellulose. 2024;31(15):9191–214. doi:10.1007/s10570-024-06125-y.
30. Ribeiro NR, Sousa MBE, Oliveira LA, de Oliveira EJ. Variability of amylose content and its correlation with the paste properties of cassava starch. PLoS One. 2024;19(10):e0309619. doi:10.1371/journal.pone.0309619.
31. Kong S, Qi W, Li X, Cao J, Xie Y, Cheng J. Clarifying the structure and characteristics of different varieties potatoes starch. Int J Biol Macromol. 2025;306(1):141631. doi:10.1016/j.ijbiomac.2025.141631.
32. Du C, Jiang F, Jiang W, Ge W, Du S. Physicochemical and structural properties of sago starch. Int J Biol Macromol. 2020;164(3):1785–93. doi:10.1016/j.ijbiomac.2020.07.310.
33. de Paula Farias V, Ascheri DPR, Ascheri JLR. Substituting corn starch with wolf's fruit and butterfly lily starches in thermopressed films: physicochemical, mechanical, and biodegradation properties. Int J Biol Macromol. 2024;281:136378. doi:10.1016/j.ijbiomac.2024.136378.
34. Shi L, Li Y, Lin L, Bian X, Wei C. Effects of variety and growing location on physicochemical properties of starch from sweet potato root tuber. Molecules. 2021;26(23):7137. doi:10.3390/molecules26237137.
35. Shi L, Guo K, Xu X, Lin L, Bian X, Wei C. Physicochemical properties of starches from sweet potato root tubers grown in natural high and low temperature soils. Food Chem X. 2024;22:101346. doi:10.1016/j.fochx.2024.101346.
36. Tafa KD, Satheesh N, Abera W. Mechanical properties of tef starch based edible films: development and process optimization. Heliyon. 2023;9(2):e13160. doi:10.1016/j.heliyon.2023.e13160.
37. Müller CMO, Laurindo JB, Yamashita F. Effect of cellulose fibers on the crystallinity and mechanical properties of starch-based films at different relative humidity values. Carbohydr Polym. 2009;77(2):293–9. doi:10.1016/j.carbpol.2008.12.030.

38. Karimi S, Abdulkhani A, Tahir PM, Dufresne A. Effect of cellulosic fiber scale on linear and non-linear mechanical performance of starch-based composites. Int J Biol Macromol. 2016;91:1040–4. doi:10.1016/j.ijbiomac.2016.06.061.
39. Kaewtatip K, Thongmee J. Studies on the structure and properties of thermoplastic starch/luffa fiber composites. Mater Des. 2012;40:314–8. doi:10.1016/j.matdes.2012.03.053.
40. Šupová M, Martynková GS, Barabaszová K. Effect of nanofillers dispersion in polymer matrices: a review. Sci Adv Mater. 2011;3:1–25.
41. Rodríguez HA, Kriven WM, Casanova H. Development of mechanical properties in dental resin composite: effect of filler size and filler aggregation state. Mater Sci Eng C. 2019;101:274–82. doi:10.1016/j.msec.2019.03.090.
42. Gutiérrez TJ, Ollier R, Alvarez VA. Surface properties of thermoplastic starch materials reinforced with natural fillers. In: Functional biopolymers. Cham, Switzerland: Springer; 2017. p. 131–58. doi:10.1007/978-3-319-66417-0_5.
43. Zare Y. Study of nanoparticles aggregation/agglomeration in polymer particulate nanocomposites by mechanical properties. Compos Part A Appl Sci Manuf. 2016;84(4):158–64. doi:10.1016/j.compositesa.2016.01.020.
44. Nilagiri Balasubramanian KB, Ramesh T. Role, effect, and influences of micro and nano-fillers on various properties of polymer matrix composites for microelectronics: a review. Polym Adv Technol. 2018;29(6):1568–85. doi:10.1002/pat.4280.
45. Olonisakin K, Fan M, Zhang X-X, Ran L, Lin W, Zhang W, et al. Key improvements in interfacial adhesion and dispersion of fibers/fillers in polymer matrix composites; focus on PLA matrix composites. Compos Interfaces. 2022;29(10):1071–120. doi:10.1080/09276440.2021.1878441.
46. Khalili H, Bahloul A, Ablouh E-H, Sehaqui H, Kassab Z, Semlali Aouragh Hassani F-Z, et al. Starch biocomposites based on cellulose microfibers and nanocrystals extracted from alfa fibers (*Stipa tenacissima*). Int J Biol Macromol. 2023;226:345–56. doi:10.1016/j.ijbiomac.2022.11.313.
47. Sanyang ML, Sapuan SM, Jawaid M, Ishak MR, Sahari J. Effect of sugar palm-derived cellulose reinforcement on the mechanical and water barrier properties of sugar palm starch biocomposite films. BioResources. 2016;11(2):4134–45. doi:10.15376/biores.11.2.4134-4145.
48. Bertuzzi MA, Armada M, Gottifredi JC. Physicochemical characterization of starch based films. J Food Eng. 2007;82(1):17–25. doi:10.1016/j.jfoodeng.2006.12.016.
49. Lee CH, Khalina A, Lee SH. Importance of interfacial adhesion condition on characterization of plant-fiber-reinforced polymer composites: a review. Polymers. 2021;13(3):438. doi:10.3390/polym13030438.
50. de Campos A, de Sena Neto AR, Rodrigues VB, Luchesi BR, Moreira FKV, Correa AC, et al. Bionanocomposites produced from cassava starch and oil palm mesocarp cellulose nanowhiskers. Carbohydr Polym. 2017;175:330–6. doi:10.1016/j.carbpol.2017.07.080.
51. Chang Y, Sun T, Fan C, Zhou X. The effect of surface modification on the properties of sisal fiber and improvement of interfacial adhesion in sisal/starch composites induced by starch nanocrystals. Compos Interfaces. 2018;25(11):981–94. doi:10.1080/09276440.2018.1450586.
52. Wei X, Tang J, Tao H, Gao W, Guo L, Cui B, et al. Correlation between interfacial adhesion and functional properties of corn stalk cellulose-reinforced corn starch-based biodegradable straws. Ind Crops Prod. 2022;189(15):115881. doi:10.1016/j.indcrop.2022.115881.
53. Cheng G, Zhou M, Wei Y, Cheng F, Zhu P. Comparison of mechanical reinforcement effects of cellulose nanocrystal, cellulose nanofiber, and microfibrillated cellulose in starch composites. Polym Compos. 2019;40(S1):e365–72. doi:10.1002/pc.24685.
54. Chen H, Miao M, Ding X. Influence of moisture absorption on the interfacial strength of bamboo/vinyl ester composites. Compos Part A Appl Sci Manuf. 2009;40(12):2013–9. doi:10.1016/j.compositesa.2009.09.003.
55. Gaidukovs S, Platnieks O, Gaidukova G, Starkova O, Barkane A, Beluns S, et al. Understanding the impact of microcrystalline cellulose modification on durability and biodegradation of highly loaded biocomposites for woody like materials applications. J Polym Environ. 2022;30(4):1435–50. doi:10.1007/s10924-021-02291-3.